

## Simple ultrashort echo time MRI measure associated with cortical bone porosity

Mahdieh Bashoor-Zadeh<sup>1</sup>, Cheng Li<sup>1</sup>, Wenli Sun<sup>1</sup>, Maite Aznarez-Sanado<sup>1</sup>, Alexander C Wright<sup>1</sup>, Antonios Zavaliangos<sup>2</sup>, and Chamith S Rajapakse<sup>1</sup>  
<sup>1</sup>University of Pennsylvania, Philadelphia, PA, United States, <sup>2</sup>Drexel University, Philadelphia, PA, United States

### Purpose:

Since cortical bone (CB) is a major contributor for the fracture susceptibility, assessment of CB quality is important in subjects at risk for diseases such as osteoporosis and renal osteodystrophy. Increased CB porosity is directly associated with decreased mechanical competence. Due to limitations in resolution and other factors, microstructure of CB pore spaces—i.e., Haversian canals, osteocyte lacunae, and canaliculi etc.—cannot be resolved by current clinical imaging modalities. Ultrashort echo time imaging (UTE) can be used to obtain proton signal from bone water which resides in pore spaces (i.e., “free” water) and bound to collagen matrix (i.e., bound water) on clinical MRI systems [1, 2]. Bound and free water, however, has direct and inverse contributions, respectively, to bone’s mechanical competence [3]. The primary purpose of this study was to derive a parameter directly associated with CB porosity using a UTE sequence that can be translated for clinical imaging.

### Methods:

**Specimens:** Cadaveric human mid tibia whole cross-sectional CB segments of thickness 36 mm were harvested from eight female donors (age range 27-97 year, mean  $\pm$  standard deviation  $62 \pm 24$  years) and stored in phosphate buffered saline (PBS) solution at 4° C prior to imaging.

**UTE Imaging:** The CB specimens underwent 3D UTE scans using a 4-channel surface coil in a 3T whole-body scanner (Siemens, Erlangen, Germany) with the following parameters: FOV = 160x160x160 mm<sup>3</sup>, TR = 12 ms, FA = 12° with 20  $\mu$ s hard pulse duration, 50000 half-projections distributed uniformly within a sphere using the method described in [4], 190 readout points per projection, gradient ramp time = 240  $\mu$ s, readout bandwidth = 125 kHz, reconstructed image matrix = 320x320x320, scan time = 10 minutes. Two acquisitions were performed with TE=50  $\mu$ s and 1200  $\mu$ s. The short-TE value was chosen to obtain the maximum proton signal resulting from free water (T2\*~3 ms), bound water (T2\*~400  $\mu$ s), and possibly from solid matrix (T2\*~60  $\mu$ s) [3, 5]. The long-TE image was acquired to have signal essentially from only free water in pore spaces because the shorter-T2\* components would have attenuated to negligible values (<5%) by 1200  $\mu$ s.

**Micro-CT Imaging:** To assess the microstructure, CB samples were imaged using micro computed tomography ( $\mu$ CT, Bruker, Kontich, Belgium) using following parameters: source voltage 100 kV, source current 100  $\mu$ A, exposure time 5.89 seconds, angular increment 0.04°, 4877 views, scan time ~ 50 hours, and isotropic voxel size 8.63  $\mu$ m.

**UTE Quantification:** CB was segmented from the background in UTE images by delineating the endosteal and periosteal boundaries using a level set based algorithm with manual adjustment when needed. Porosity index was defined as the ratio of mean CB intensity in the 1200- $\mu$ s image to that of 50- $\mu$ s image.

**Micro-CT Quantification:** The solid phase of CB was segmented from the background and pore spaces by selecting a threshold value at the midpoint of the two peaks corresponding to bone tissue and pores of the intensity histogram. Volume of each pore was calculated using a 3D object counting algorithm described in [6]. CB porosity was defined as the ratio of total pore volume (excluding the pore spaces connected to the marrow cavity) over total CB volume.

### Results:

Generally increased CB porosity in the older compared to younger subjects was visually evident from the micro-CT images (**Figure 1**). Micro-CT derived CB porosity was highly correlated with UTE-derived porosity index ( $R^2 = 0.85$ ). The association between age and porosity index was moderate ( $R^2=0.22$ ).

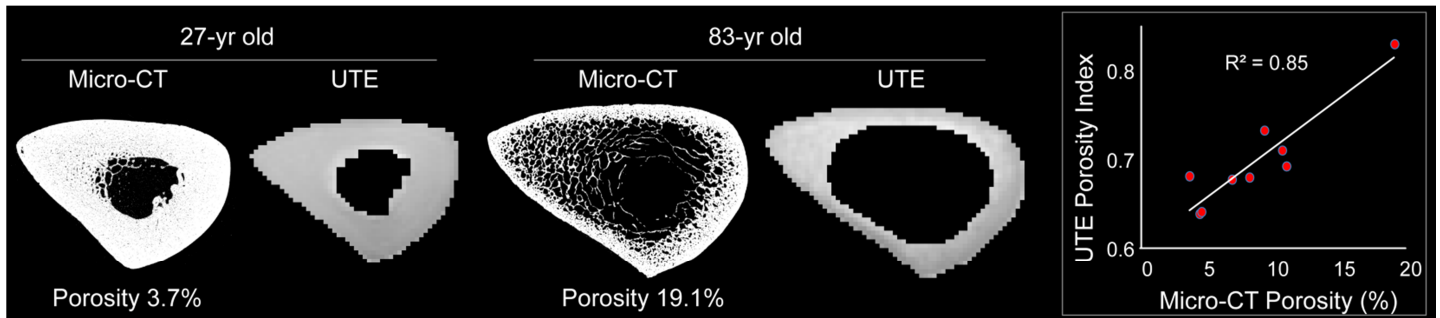


**Figure 1:** Comparison of mid-slice micro-CT and UTE CB images of a young (left panel) and older (middle panel) subject; and association between micro-CT derived CB porosity and UTE-derived porosity index (right panel).

### Discussion:

The high correlation between UTE-derived porosity index and reference porosity values obtained from high-resolution micro-CT images suggests that CB porosity can be assessed using a clinically feasible UTE sequence without assuming average T2\* values for bound and free water distributions. While the utilized micro-CT image resolution is sufficient to resolve Haversian canals (size 27-76  $\mu$ m [7]), only a portion of osteocyte lacunae (size 2-30  $\mu$ m [8]) was captured resulting in slight underestimation of micro-CT derived porosity. The contribution to porosity index from canaliculi space may be negligible because the fluid volume in canaliculi is less than 5% of osteocyte lacunae [9]. Finally, one reason for only a moderate correlation between age and porosity could be due to the fact that age-related changes in CB porosity is related predominantly to Haversian canals, whereas the porosity of osteocytic lacunae are thought to be independent of age [7].

### Conclusions:

UTE-derived porosity index could be used to enhance MRI-based finite-element predictions of CB strength in humans. Further calibrations are needed to convert porosity index into porosity values.

**References:** [1] Techawiboonwong et al. Radiology 248(3):824-33 (2008). [2] Du J Magn Reson. 207(2):304-11 (2010). [3] Horch et al. PLoS One. 21;6(1):e16359 (2011). [4] Wong et al. MRM 32(6):778-784 (1994). [5] Du et al. Magn Reson Med. Epub ahead of print (2012). [6] Bolte et al. J. Microsc. 224:213–232 (2006). [7] Wang et al. J Orthop Res. 21(2):312-9 (2003). [8] McCreddie et al. J Biomech. 37(4):563-72 (2004). [9] Wang et al. Proc Natl Acad Sci U S A. 16;102(33):11911-6 (2005).

**Acknowledgements:** NIH grant K25 AR 060283.